ECHAHID HAMMA LAKHDAR UNIVERSITY - EL-OUED
Under the Supervision of the DGRSDT and in collaboration with the CRTI
International Pluridisciplinary PhD Meeting (IPPM'20)
23-26, 2020 1st Edition, February
Theme: Modern Technology and Fineness Life

4 to 5 pages

Aerodynamic performances of a moving H-Darrieus-type vertical-axis wind turbine

Farouk Meguellati*, Fateh Ferroudji*, Lakhdar Saihi*, Adel Messaoudène**, Khaled Koussa*, Khayra Roummani*, Youcef Bakou*

* Unité de Recherche en Energies Renouvelables en Milieu Saharien, URERMS, Centre de Développement des Energies Renouvelables, CDER, 01000, Adrar, Algeria
** Laboratoire d'Etude des Systèmes Energétiques Industriels, Département de Mécanique, Faculté de Technologie, Université Batna2, Algeria
E-mail: farouksdz@yahoo.fr, fferroudji@yahoo.fr, sadysaihi@live.fr, ado.messaoudene@yahoo.fr, koussakhaled@gmail.com, khayra.roummani@univ-usto.dz, youcefbakou@gmail.com

Abstract

This study aims to investigate numerically a 10 kW straight-bladed Darrieus type Vertical Axis Wind Turbine (VAWT) by using fluent 6.3.26 . A symmetry NACA0018 aerofoil shape is used for the wind turbine blades. The simulations are carried out by solving the 2D Reynolds Averaged Navier-Stokes (RANS) equations in addition to the realizable k-ϵ turbulence model. The enhanced wall treatment algorithm is adopted near solid boundaries with a maximum y^+ of 3. The effect of solidity (in terms of chord length) on the blade's aerodynamic performances (lift, drag and moment coefficients) of the turbine is evaluated. Computed results show that during one revolution, the blade with a small chord length presents low moment coefficient in a range of [60°-120°] while it is higher in the range of [200°-325°] in comparison to other cases.

Keywords: lift coefficient, drag coefficient, CFD simulation, sliding mesh, enhanced wall treatment, turbulence modelling.

1. Introduction

In recent years, Due to the diminution of fossil fuel resources and the increasing conscience for the necessity of a renewable energy source, wind power amongst all other clean energies is important player in the global energy market, which is growing speedily. According to BP Statistical Review of World Energy report from 2019, the global installed capacity reached 591GW at the end of 2018 (an increase of 9%) [1].

A wind turbine is a device which extracts the kinetic energy from the atmospheric wind flows, converting it into a torque on the rotor, which is connected to the main shaft and spins a generator to create electricity [2]. These devices can be divided mainly into two groups: horizontal axis wind turbine (HAWT) and vertical axis wind turbine (VAWT) types. The first group is the most widely available in the field of large-scale power generation. Compared to HAWT designs the Darrieus machine which has various forms, including H-type and Φ-type, offers many distinct advantages including accessibility (for example, the primary bearings and generator may be located at or close to the ground), low noise, and simple blade design [3].

In the current study, the commercial CFD solver Fluent 6.3.26. was employed as a standalone simulation environment. A 2D transient CFD simulation resolving Reynolds Averaged Navier-Stokes (RANS) equations in addition to the realizable k-ϵ turbulence model is carried out[4].

2. CFD model setup

2.1. Model geometry

In the present study, the turbine blade consisting of NACA0018 airfoil with several chord lengths (c), 0.47m, 0.53m and 0.6m, was employed.

The computational domain was divided into two regions: a circular inner domain for the rotating region and a rectangular outer domain for the stationary region (Fig. 1). A sensitivity analysis was used to determine the outer computational domain, yielding dimensions of $20R$ in the two directions parallel and perpendicular to the free-stream, respectively. These dimensions avoid any blockage effect and allow the rotor to reach a fully developed state.

The turbine rotor center was located $10R$ from the inlet and the radius of the rotating region enclosing the rotor was specified to be $1.25R$. Table 1 gives a detailed description of the reference rotor configuration.

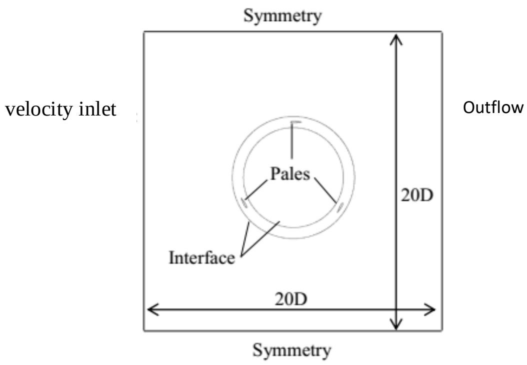

Fig.1. Geometric description of the computational domain**.**

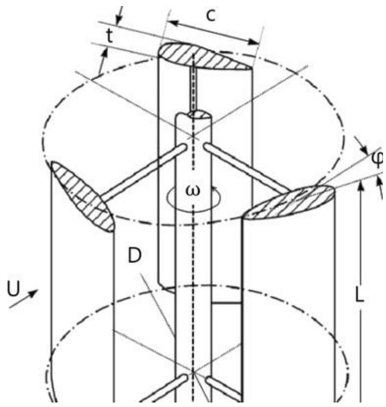

Fig. 2. 3D view of straight-bladed Darrieus wind turbine**.**

Table 1. Description of turbine configuration [1]

Blade profile	NACA 0018
Blade number	3
Blade chord length *c* [m]	0.47, 0.53, 0.60
Rotor diameter D [m]	8.9
Rotor height L [m]	7.6
Aspect Ratio *AR=L/D*	0.85

2.2. Dimensionless performance parameters

For the performance evaluation of the VAWT under investigation, the following non-dimensional parameters are used.

Tip speed ratio (TSR), λ which is calculated from:

$$\lambda = \frac{\omega R}{U_\infty} \quad (1)$$

In the previous equation, ω is the rotational speed in (rad·s^{-1}), R is the radius of the rotor in (m), and U_∞ is the unperturbed wind speed (10 m·s^{-1} in this case).

The angle of attack (AoA) α has a simple relation with the azimuth angle θ, as well as the tip speed ratio λ (Eq. 2). The analysis of this equation can be derived from the velocity triangle analysis (Fig.3), as follow:

$$\alpha = \tan^{-1}\left[\frac{V_n}{V_c}\right] = \tan^{-1}\left[\frac{U_\infty \sin\theta}{U_\infty(\lambda + \cos\theta)}\right] \quad (2)$$

$$w = \sqrt{V_n^2 + V_c^2} \quad (3)$$

Where V_c represents the chordal velocity component and V_n represents the normal velocity component, hence w is the relative velocity.

The pitch angle φ (zero in this study) is the angle between the chord axis and the blade tangential path (Fig.2 a).

Several aerodynamic forces will be generated on the aerofoil due to the wind flow over the turbine blades. These forces mainly are drag and lift forces and are function of the incidence angle (AoA) α of the flow. By resolving these forces, the perpendicular force F_N and the tangential force F_T (responsible force of the torque and power output) are acquired as in Fig.2.

Another essential parameter affects the forces on the sectional aerofoil is the turbine solidity. It can be calculated as:

$$\sigma = \frac{Nc}{2R} \quad (4)$$

Power coefficients are calculated as follows:

$$C_p = \frac{P}{\frac{1}{2}\rho A U_\infty^3} \quad (5)$$

Dynamic torque coefficient (C_T) is define as:

$$C_T = \frac{T}{\frac{1}{2}\rho A R U_{\infty}^{3}} \quad (6)$$

where P is the power (W), T is the dynamic torque (N·m), respectively,ρ is the air density in (kg·m^{-3}), and A is the swept area (m^2).

2.3. Meshing topology

The way in which the grid is generated has a strong impact on the model's accuracy, and many considerations must be followed. Of particular importance is modelling the boundary layer in sufficient detail by covering relevant boundaries with at least 10 layers of cells; this allows the chosen turbulence model to achieve its calibrated performance [4]. Accordingly, the grid used in the present work had 45 layers of quadrilateral cells, with a first cell height of about 10^{-5}m and a growth rate of 1.135 near the aerofoil boundary (Fig. 4).

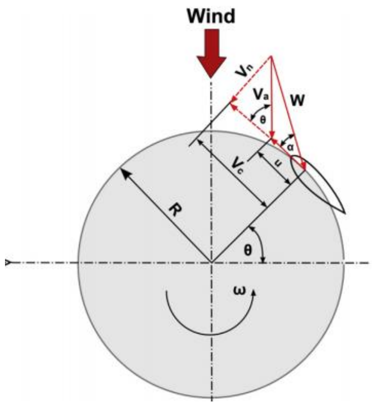

Fig.3. top view projection of fig. 2**.**

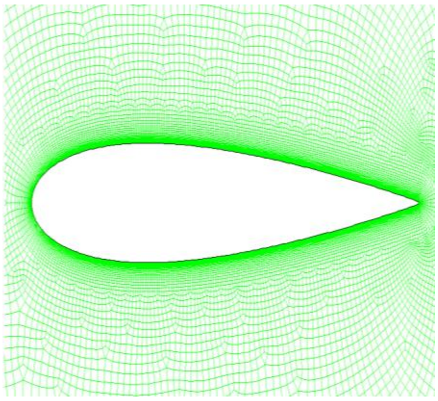

Fig. 4. Boundary layer on blade surface and mesh distribution**.**

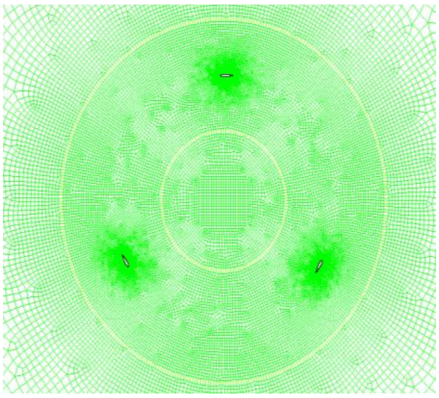

Fig.5. close view of the rotating inner domain**.**

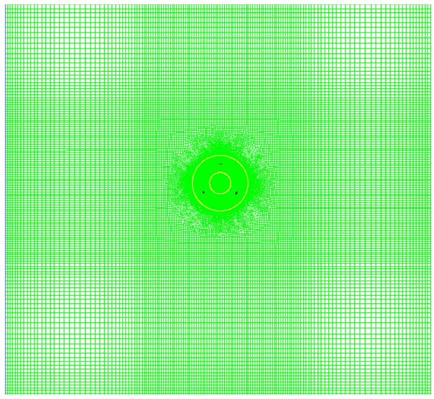

Fig. 6. view of the entire domain**.**

Beyond the inflation region, an unstructured mesh was employed for the rotating region whereas a structured mesh for the stationary region is adopted. To minimize the dissipation of the turbulent structures, the maximum edge length used for the mesh cells in the rotating region was 0.1m (Fig. 4). Because the study aimed to investigate the effect of solidity (in terms of chord length), the number of elements in the rotating domain is changing, whereas a number of 28,000 elements in the stationary domain was generated using pre-processor GAMBIT 2.4 Design Modeller.

Moreover, to ensure the quality of the reference configuration (NACA0018) mesh, maximum element skewness was measured beyond the inflation layer and was found to be 0.7 which illustrate the excellent quality of the grid [4]

2.4. Boundary conditions

A velocity inlet was placed on the left side of the computational domain and was defined to have a uniform velocity profile of 10 m.s^{-1} [1]. In fully developed flows, the turbulence intensity may be as high as a few percent depending on the Reynolds number [4]. In the present work, a turbulent intensity of 3%, and turbulent length scale of 0.3115 were selected [4]. An outflow boundary condition was prescribed at the right side since details of the flow velocity and pressure at the exit are not known. This boundary condition type updates the outflow velocity and pressure in a manner that is consistent with a fully-developed flow assumption [4]. Also, a symmetry boundary condition was applied to the top and bottom edges of the domain for the purpose of neglecting solid blockage effects [5], and the blade surfaces were regarded as no-slip wall boundaries.

The inner rotating region was attached to the outer region by employing a sliding mesh technique, which conserves mass and momentum through an interface boundary condition type.

2.5. Turbulence modelling

In the present work, two-equation Realizable k-ε turbulence model among others, thought to be the widely used turbulence model for industrial applications [4]. It provides superior performance for flows involving rotation, boundary layers under strong adverse pressure gradients, separation, and recirculation [4].

2.6. Simulation parameters

In all cases in this work, the air density and viscosity were set to 1.225 kg m^3 and $1.78x10^{-5}$ $kg.m^{-1}.s^{-1}$, respectively. A pressure based solver called SIMPLE, with an absolute velocity formulation, was applied, in which velocity and pressure are coupled with a segregated algorithm, and the governing equations are solved iteratively by the Gauss-Seidel algorithm for the entire flow domain. The PRESTO! spatial discretization scheme was used to solve the pressure equation, while for the other variables the second order scheme was adopted.

In the dynamic simulation, the inner region is moving with a constant rotational velocity ω, calculated from eq.(1) for different values of TSR λ. A time step correspond to an angular rotation of 1° was used.

All simulations were carried out by means of a parallel processing (64-bit, 1.6 GHz Core i5 processor, 6 GB RAM) and the residual convergence criterion was set to $1x10^{-4}$ for all variables.

3. Results and discussion

In this section, a validation curve (Castelli *et al.* [6], fig.7) as well as aerodynamic performances (figs.8,9, 10, 11 and 12) of one blade will be presented.

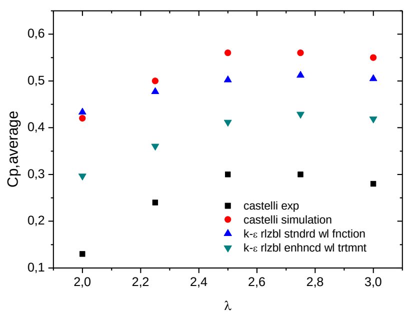

Fig.7. The average power coefficient as a function of tip speed ratio**.**

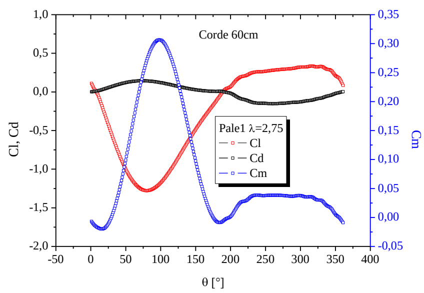

Fig.8. aerodynamic performances of blade1 at λ=2.5**.**

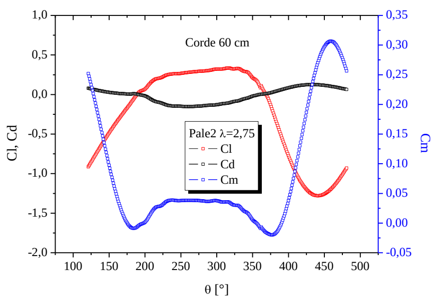

Fig.9. aerodynamic performances of blade2 at λ=2.5**.**

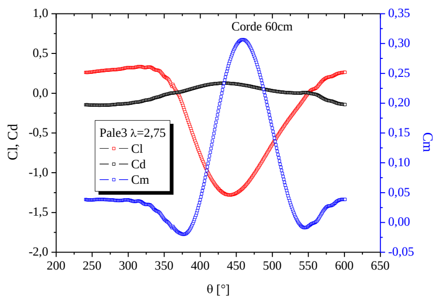

Fig. 10. aerodynamic performances of blade3 at λ=2.5**.**

Figure 7 presents a validation curve with literature of power coefficient with respect to tip speed ratio. A good agreement was observed between experimental [6] and our numerical study when using enhanced wall treatment. While figures 8, 9 and 10 represent the aerodynamic performances of each blade of the wind turbine for the chord length 0.6m.

In figures 11 and 12 the moment coefficient for the study cases is presented for the blade 1 and 2. It could be noted that the case of the lowest chord length present a minimum moment coefficient for the bell shaped part of the curve while the inverse phenomenon is observed in the rest of the curve and vice versa for the other two cases.

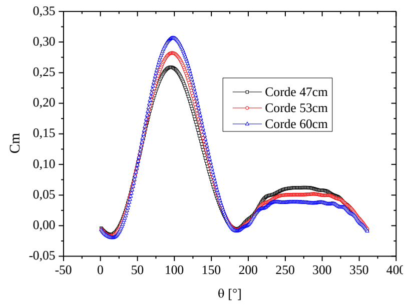

Fig.11. moment coefficient at λ=2.5 for studied cases of blade 1**.**

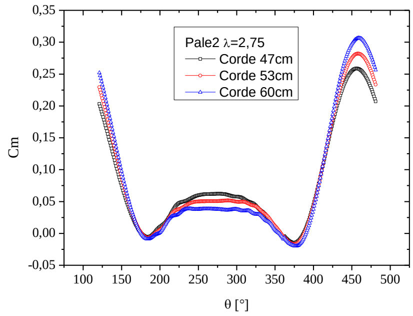

Fig. 12. moment coefficient at λ=2.5 for studied cases of blade 2**.**

4. Conclusion

In this paper, a numerical simulation of unsteady Reynolds averaged Navier-Stokes (URANS) of the flow around an H-Darrieus wind turbine, is carried out by using Fluent 6.3.26 in addition to the pre-processor Gambit 2.4. The Realizable k-ε turbulence model is used in addition the enhanced wall treatment near the solid boundaries. The sliding mesh model is adopted for the moving zone to simulate the revolution of the wind turbine. A good agreement of our process with literature was observed. The effect of solidity on the aerodynamic performances showed that the increase of solidity presents a high moment coefficient in an angular range of 200° with a mean value of 0.15 while in subsequent angular range it presents a low moment coefficient having a mean value of 0.01.

References

1. Ferroudji, F., Khelifi C., Meguellati F., Koussa K., Design and Static Structural Analysis of a 2.5 kW Combined Darrieus-Savonius Wind Turbine, *International Journal of Engineering Research in Africa*, 30, 2017, 94-99.
2. B. Dudley, BP Statistical Review of World Energy, 68th ed.; BP: London, UK, 2019.
3. Ferroudji, F, Cherif Khelifi, C., Meguellati, F., Modal Analysis of a Small H-Darrieus Wind Turbine Based on 3D CAD, FEA, *International Journal of Renewable Energy Research*, Vol.6 (2), 2016.
4. Fluent, Fluent 6.3 User's Guide, Fluent Inc., NH, USA, 2006.
5. Zhang LX, Liang YB, Liu XH, Jiao QF, Guo J. Aerodynamic performance prediction of straight-bladed vertical axis wind turbine based on CFD. Adv Mech Eng 2013;5.
6. M. R. Castelli, Alessandro E., Ernesto B. The Darrieus wind turbine: Proposal for a new performance prediction model based on CFD. Energy 36 (2011) 4919-4934.